

Research Article

Superconductivity and Structural of the New Er358 Materials

Thitipong Kruaehong^{1,*}, Supphadate Sujinnapram², Somkid Sinwittayarak³
Tunyanop Nilkamjon⁴, Sermsuk Ratreng⁴, and Pongkaew Udomsamuthirun⁴

Received: 1 March 2023

Revised: 13 May 2023

Accepted: 16 May 2023

ABSTRACT

The Er358 superconductor was synthesized via the standard solid-state reaction method and demonstrated an average onset critical temperature of 95.48 K and an offset critical temperature of 89.70 K. Its crystal structure was classified into two groups: superconducting and non-superconducting compounds, possessing orthorhombic structures corresponding to the Pmmm and Pbnm space groups, respectively. The ratio of superconducting to non-superconducting compounds was 1:2, and their respective lattice parameters were $a=3.8248 \text{ \AA}$, $b=3.8770 \text{ \AA}$, $c=31.666 \text{ \AA}$, and $a=7.1006 \text{ \AA}$, $b=12.139 \text{ \AA}$, $c=5.6418 \text{ \AA}$. The samples exhibited smooth and dense surfaces, and their element distribution was analyzed via EDX mapping. The $\text{Cu}^{2+}/\text{Cu}^{3+}$ ratio was 0.0527, and the oxygen content deficiency was 0.300. The oxygen content was determined to be 17.7 using iodometric titration. Additionally, two endothermic peaks were observed in the heat reaction at 935°C and 1,050°C.

Keywords: Er358, New Er-based Superconductors, X-ray diffraction.

¹ Department of industrial electric, Faculty of Science and Technology, Suratthani Rajabhat University, Suratthani 84100, Thailand.

² Department of Physics, Faculty of Liberal Arts and Science, Kasetsart University, Kamphaeng Saen Campus, Nakhon Pathom 73140, Thailand.

³ Department of Computer Science, Faculty of Science and Technology, Suratthani Rajabhat University, Suratthani 84100, Thailand.

⁴ Prasanmitr Physics Research, Department of Physics, Faculty of Science, Srinakharinwirot University, Bangkok 10110, Thailand.

* Corresponding author, email: thitipong.kru@sru.ac.th

Introduction

In 1986, Bednorz and Muller [1] synthesized the first cuprate superconducting material, $\text{La}_2\text{BaCuO}_4$ (La214) compound, with a critical transition temperature above 35 K. The following year, Chu et al. [2] replaced the La^{3+} ion in La214 with Y^{3+} in the BaCuO_2 perovskite structure. This change resulted in a smaller atomic radius of Y^{3+} and increased the critical temperature of Y123 to 93 K. Over the past two decades, the YBaCuO family, including Y124 [3] and Y247 [4], has been discovered and researched. These compounds have different arrangements of CuO_2 planes [5] and Cu-O chains [6] in their crystal structures. Electron pairs are generated in the CuO_2 planes and Cu-O chains, which act as carrier reservoirs for superconductivity. The critical temperature of cuprate superconductors increases with the number of CuO_2 planes and Cu-O chains [7]. La214 has one CuO_2 plane [8], while Y123 has two CuO_2 planes and one chain [9].

Alibadi et al. [10] recently developed a new superconducting material in Y358 that showed an increased critical temperature of 102 K, with lattice parameters $a=3.8880 \text{ \AA}$, $b=3.8230 \text{ \AA}$, and $c=31.013 \text{ \AA}$. While lattice parameters a and b were similar to Y123, while parameter c increased three times greater. This led to an increase in Cu-O chains, CuO_2 planes, and the critical temperature (T_c) in Y358. Taviana and Akhavan [11] analyzed the band structure of Y358 and found that it had five CuO_2 planes and three CuO chains [12], which contributed to the increase in temperature. Additionally, Udomsamuthirun et al. [13] proposed that the absence of a Y-atom in the crystal structure of Y358 resulted in 20% more convenient space conductivity than Y123. An increase in temperature of approximately 10 K in Y358 was significant in the YBaCuO family. Furthermore, the oxygen content in the crystal structure also played an essential role in determining the critical temperature [14].

Y-based superconductors are categorized in the RE123 system, where RE refers to rare earth elements, including Y, Dy, Er, and others. Among these, Er-based superconducting materials are particularly interesting [15-17]. In 2009, Kruaehong et al. [18] synthesized bulk Er123 superconductor using a solid-state reaction method, with Er_2O_3 , BaCO_3 , and CuO mixed in the appropriate 1:2:3 stoichiometric ratio. The resulting sample showed a critical temperature of 93 K, which is similar to Y123. The Rietveld method [19] was used to characterize the phase composition. The samples had two phases; a superconducting phase with an orthorhombic structure of $a=3.8186 \text{ \AA}$, $b=3.8835 \text{ \AA}$, and $c=11.682 \text{ \AA}$, and Pmmm space group. The second phase was a non-superconducting phase (BaCuO_2) with a cubic structure of $a=b=c=18.24617 \text{ \AA}$ and Im-3m space group. The percentage of superconducting phase and non-superconducting phase was 91% and 9%, respectively. The $\text{Cu}^{3+}/\text{Cu}^{2+}$ ratio and oxygen content of the sample were characterized using the iodometric titration method, and the values were found to be 0.289 and 6.84, respectively. Kita et al. [20] synthesized bulk Er123 samples using the solid-state reaction method. Er_2O_3 (99.9%), BaCO_3 (99.95%), and CuO (99.99%) were mixed and ground. The resulting powder was calcined twice at 1,173 K for 12 hours in air, with intermediate regrinding. The powder was pressed into pellets and sintered at 1,233 K for 12 hours. The critical temperature of the samples was measured using the standard four-probe technique for electrical resistivity and found to be about 92 K. Similarly, Hassan and Yahya [21] prepared bulk Er123 samples using the

conventional solid-state reaction method with high-purity Er_2O_3 , BaCO_3 , and CuO . The powders were calcined at 900°C for 48 hours, with several intermediate grinding steps. The powders were reground, pressed into pellets, and sintered at 900°C for 24 hours. The crystal structure of Er123 is orthorhombic with a Pmmm space group, and the lattice parameters are $a=3.8140\text{ \AA}$, $b=3.8820\text{ \AA}$, and $c=11.675\text{ \AA}$. The grain size of the samples ranges from 2-10 μm , and porosity occurs in the samples.

In 2006, Nazarova et al. [22], The Er123 was synthesized using a solid-state reaction method, with a calcination process at 900°C and 930°C for 21 hours, sintering at 950°C for 23 hours, and annealing at 450°C for 23 hours. The lattice parameters of Er123 were characterized using X-ray powder diffraction analysis, with $a=3.8164\text{ \AA}$, $b=3.8868\text{ \AA}$, and $c=11.661\text{ \AA}$, and the critical temperature was found to be 92 K using AC magnetic susceptibility. Given the similarities in physical properties between Y-based and Er-based superconductors, we suggest that replacing Er-atoms with Y-atoms in Y358 superconductor may lead to the discovery of superconductivity in this material. In this study, we aim to fabricate Er358 superconductors using solid-state reaction and measure their physical properties using four-probe (DC), Powder X-ray diffraction, EDX with mapping technique, and iodometric titration.

Materials and Methods

Er358 was produced by synthesizing a sample through a solid-state reaction method that utilized 99.99% pure of Er_2O_3 , BaCO_3 , and CuO precursors in a 3:5:8 ratio. The initial composition of $\text{Er}_3\text{Ba}_5\text{Cu}_8\text{O}_{18.8}$ was mixed. The resulting powders were heated for 24 hours at 950°C with twice intermediate grinding, and the furnace was then cooled. The powders were ground and pressed into pellets approximately 30 mm in diameter and 3 mm thick, which were then heated at 950°C in air for 24 hours. The DC electrical resistance versus temperature was measured using the four-point probes method with silver paste contact. The samples were analyzed using power X-ray diffraction with $\text{CuK}\alpha$ radiation on a D8 Discovery diffraction. Elementary analysis was conducted using EDX mapping techniques, and micrographs were taken using a FEI Quanta400 and attached Scanning Electron Microscope (SEM). The melting point temperature was determined using the Perkin Elmer DTA7 model. The Cu^{2+} and Cu^{3+} values, ratio of $\text{Cu}^{2+}/\text{Cu}^{3+}$, and oxygen content were determined using the iodometric titration method [23-27].

Results and Discussion

To measure the superconductivity temperature of the cylindrical specimen, resistivity versus temperature was measured using the four-probes measurement with a constant current of 200 mA, 250 mA, and 300 mA, respectively. The temperature was measured between 77 K and 120 K using a type K thermocouple as the temperature sensor. The onset temperature of superconducting transition (T_c onset) and the zero-resistivity temperature (T_c offset) were determined. The electrical resistivity dependence temperature of the bulk Er358 samples is shown in Figure 1. The critical temperature duration temperature was measured using a constant current of 200 mA, 250 mA, and 300 mA. The values of T_c onset (95.97 K, 95.43 K, and 95.04 K) and T_c offset (90.31 K, 89.78 K, and 89.01 K)

were obtained from the curve using these currents, respectively. In 2008, Naito et al. [28] synthesized bulk Er123 and measured the critical temperature using the conventional four-terminal method with a current density of 0.1 A/cm^2 . We found that the critical temperature increased with longer annealing processed time, which could also control the oxygen deficiency in the samples.

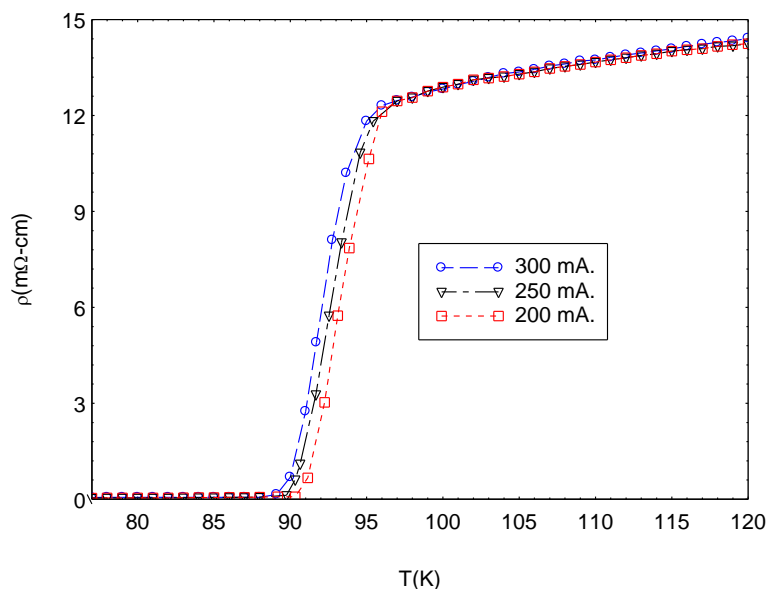


Figure 1 The resistivity versus temperature of Er358 bulk sample.

Er358 superconductor samples underwent structural analysis through X-ray powder diffraction (XRD) using a $\text{CuK}\alpha$ target to produce a beam of a single wavelength (1.5406 \AA). The samples were scanned within the range of $2\theta = 10^\circ\text{-}90^\circ$, with an angle increment of 0.05° and a scan speed of $1^\circ/\text{min}$, all at room temperature. The pressed powder for XRD was subjected to 40 kV and 30 mA. The lattice parameter and pattern of XRD of the phase composition were refined using Rietveld software program.

The XRD patterns showed that the samples contained a mixture of superconducting and non-superconducting compounds, as seen in Figure 2 the percentage of the superconducting compound was 32.32%, corresponding to the Pmmm space group, while the non-superconducting compound was 67.68%, corresponding to the Pbnm space group. The superconducting compound had an orthorhombic structure [29] with lattice constants $a=3.8248 \text{ \AA}$, $b=3.8770 \text{ \AA}$, and $c=31.666 \text{ \AA}$ and a cell volume of $V=469.57 \text{ \AA}^3$. The non-superconducting sample also had an orthorhombic structure with lattice constants $a=7.1006 \text{ \AA}$, $b=12.139 \text{ \AA}$, and $c=5.6418 \text{ \AA}$.

The green vertical tick marks on the XRD patterns indicated the phase composition of the samples, with the first mark representing the superconducting compound and the second mark representing the non-superconducting compound. The blue line at the bottom of the patterns showed the difference between the experimental and calculated data, with the maximum difference occurring at about 32° . The black solid line represented the raw experimental data, while the red circles represented the calculated data.

The orthorhombicity [30] of a crystal structure is a measure of the degree to which the three axes of the unit cell deviate from being mutually perpendicular. In this case, the orthorhombicity of Y358 and Er358 was calculated using the formula $200 (b-a)/(b+a)$, where a and b are the lattice parameters of the crystal structure along two of the orthogonal axes. The orthorhombicity values obtained were 1.70% for Y358 and 1.35% for Er358. This indicates that the crystal structure of Er358 is slightly more stable than that of Y358, as the difference in orthorhombicity between the two compounds is only 0.35%.

The mass density of a material is its mass per unit volume. The theoretical mass density of Er358 was calculated to be 6.1 g/cm^3 . However, the experimental mass density of the sample was found to be about 5.3 g/cm^3 . This difference in mass density suggests that there may be some porosity in the surface of the sample, which would reduce its mass density.

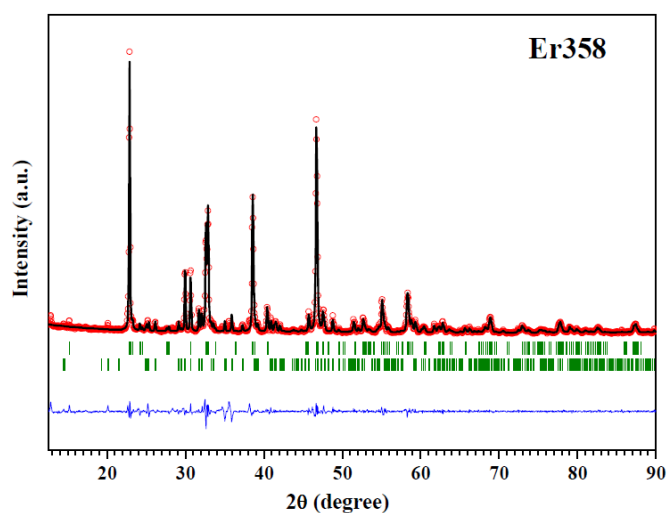


Figure 2 Rietveld refinement XRD pattern of Er358 superconductor.

The EDX mapping technique was used to investigate the microstructure and chemical analysis of the Er358 superconductor samples. The first micrograph shows the surface morphology image of the samples, while the second to fourth micrographs show the element composition in the samples. The samples exhibit four elements consisting of Er, Ba, Cu, and O, which appear in yellow, red, blue, and green, respectively. No impurities were found in any of the samples.

The surface of the samples appears smooth and dense, with grain sizes that are connected and randomly oriented. In Figure 3 (a), all elements exhibit homogeneous distribution, while in Figures 3 (b) and (c), all elements show an inhomogeneous distribution.

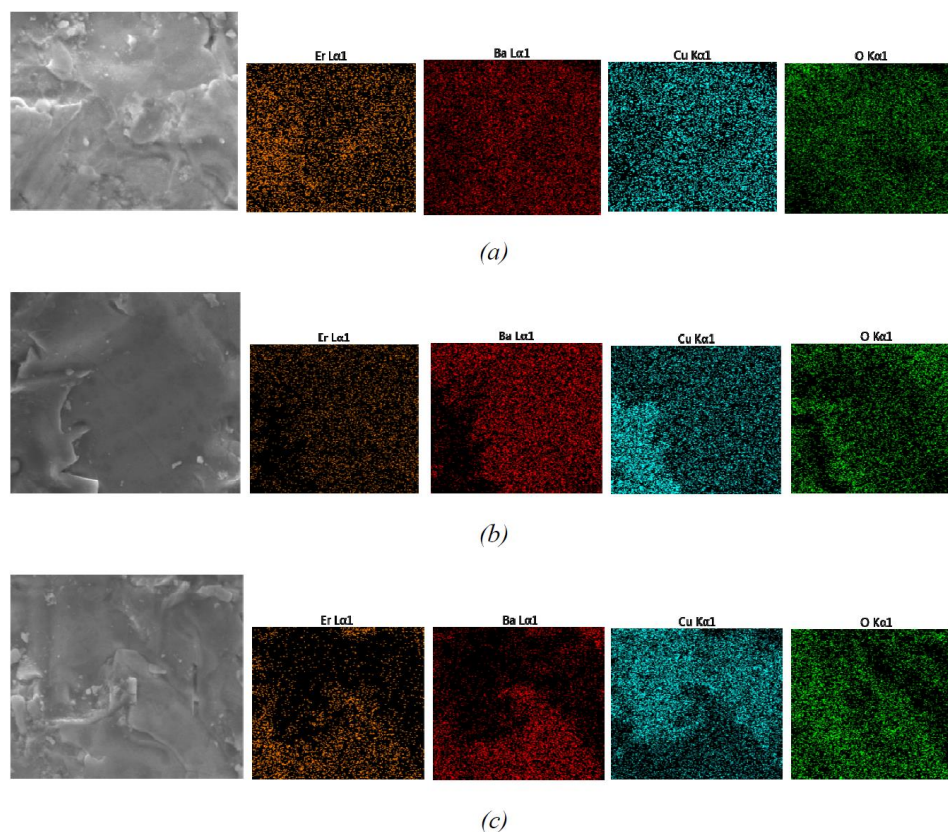


Figure 3 EDX mapping micrograph of Er358 superconductor.

The ratio of $\text{Cu}^{2+}/\text{Cu}^{3+}$ and oxygen content deficiency (δ) are important factors that can affect the crystal structure. The mechanism of superconductivity in cuprate superconductors depends on the distribution of Cu^{2+} and Cu^{3+} in the octahedral site, which are in the $3d^9$ and $3d^8$ configurations, respectively [31]. In this case, the compound of Er358 has a $\text{Cu}^{2+}/\text{Cu}^{3+}$ ratio of 0.0527, a δ value of 0.300, and an oxygen content of 17.7. The δ value plays a role in determining the crystal structure of the material. For example, when the δ value of Y123 ranges from 1 to 0.5, the material has a tetragonal structure [32] and exhibits semiconducting behavior. At $\delta=0.51$, the Y123 material transitions from a tetragonal structure to an orthorhombic structure, and at $\delta=0.2$, the material enters the superconducting state. When $\delta=0$, the Y123 material has a perfect orthorhombic structure and a critical temperature transition above 90 K.

The sintering temperature was determined from operating the Perkin Elmer DTA7 model. The heating process involved starting at room temperature and gradually increasing the temperature at a rate of $20^\circ\text{C}/\text{min}$ until 940°C . The heating rate was then reduced to $2^\circ\text{C}/\text{min}$ from 941°C - 1200°C , and the decomposition temperature occurred in this range. Two peaks were observed during the heating process, with the first peak indicating the transformation from the solid state to the liquid phase at 935°C , and the second peak occurring at $1,050^\circ\text{C}$. The XRD analysis showed that the second phase was Er211 ($\text{Er}_2\text{BaCuO}_5$), which was the second phase of Er123.

The precursor powder of Y123 reported by Feng et al. [33], the first endothermic peak in the DTA curve occurred at 952°C , and the second endothermic peak at 1022°C . However, other studies by

Kim et al. [34] and Langhorn et al. [35] showed that the first endothermic peak corresponded to the formation of the non-superconducting compound Y211 and the liquid compound. Based on the XRD analysis, it was believed that Y123 was stable and formed in the solid state under a sintering temperature of 920°C.

The surface morphology of the Er358 bulk sample showed defects and inhomogeneity. The resistivity properties of Er358 are similar to those of Y123. In order to achieve a higher critical temperature, it is necessary to create holes in the Cu-O chain and oxygen at the CuO₂ plane. Increasing the number of chains and planes in the crystal structure is important for achieving a higher critical temperature in this material. In 1987, Nakajima et al. [36] proposed that in high-temperature superconductors, increasing the number of CuO₂ planes was limited to three. The Er358 superconductor synthesized in this paper was not doped. Improving the physical properties may require a longer annealing process and substitution of the metals in the crystal structure to increase the current transport in these materials.

Conclusions

The new stoichiometry of the Er358 superconducting material compound was synthesized using the standard solid-state reaction method. The compound exhibited onset critical temperatures of 95.97 K, 95.43 K, and 95.04 K, and offset critical temperatures of 90.31 K, 89.78 K, and 89.01 K. The compound had an orthorhombic structure with lattice parameters of $a = 3.8248 \text{ \AA}$, $b = 3.8770 \text{ \AA}$, and $c = 31.666 \text{ \AA}$, and a space group of Pmmm. In contrast, the non-superconducting compound had lattice parameters of $a = 7.1006 \text{ \AA}$, $b = 12.139 \text{ \AA}$, and $c = 5.6418 \text{ \AA}$, and a space group of Pbnm. The superconducting compound accounted for approximately one-third of the total compound, and its orthorhombicity was 1.70%. The compound exhibited a homogenous, smooth, and dense surface morphology, with random grain size and orientation. All elements were uniformly distributed without any impurities. The ratio of Cu²⁺/Cu³⁺ was 0.0527, and the oxygen content deficiency (δ) was 0.300, with an oxygen content of 17.7, as determined by the iodometric titration method. The compound's decomposition temperature was measured using Differential Thermal Analysis and exhibited two peaks at 935°C and 1,050°C, respectively, indicating an endothermic reaction.

Acknowledgements

This work was supported in part by Research and Development institute of Suratthani Rajabhat University. Supports from Department of Physics, Srinakharinwirot University are acknowledged.

References

1. Bednorz JG, Müller KA. Possible high T_c superconductivity in the Ba-La-Cu-O System. *Z Phys B Con Mat.* 1986;64(2):189-93.
2. Wu MK, Ashburn JR, Torng C, Hor PH, Meng RL, Gao L, et al. Superconductivity at 93 K in a new mixed-phase Y-Ba-Cu-O compound system at ambient pressure. *Phys Rev Lett.* 1987;58(9):908-10.
3. Marsh P, Fleming RM, Mandich ML, DeSantolo AM, Kwo J, Hong M, et al. Crystal structure of the 80 K superconductor $YBa_2Cu_4O_8$. *Nature.* 1988;334:141-3.
4. Bordet P, Chailout C, Chenavas J, Hodeau JL, Marezio M, Karpinski J, et al. Structure determination of the new high-temperature superconductor $Y_2Ba_4Cu_7O_{14+x}$. *Nature.* 1988;334:596-8.
5. Yamauchi H, Karppinen M. Hole-doping of the CuO_2 planes in high T_c superconductors. *Mater Sci Eng B.* 1998;54:92-7.
6. Matic VM, Lazarov ND. Geometric distribution of CuO chains in $YBa_2Cu_3O_{6+x}$. *Phys C: Supercond Appl.* 2006;443(1-2):49-56.
7. Sanna S, Manca P, Agrestini S, Saini NL, Bianconi A. Anisotropic in plain Cu-O strain and the stripe quantum critical point in $YBa_2Cu_3O_{6+k}$. *Int J Mod Phys B.* 2000;14(29n31):3668-72.
8. Basov DN, Woods SI, Katz AS, Singley EJ, Dynes RC, Xu M, et al. Sum rules and interlayer conductivity of high- T_c cuprates. *Science.* 1999;283(5398):49-52.
9. Govind, Ajay, Tripathi RS. Superconducting properties of bilayer cuprates: role of CuO chains. *Phys C: Supercond Appl.* 2000;334(3-4):215-28.
10. Aliabadi A, Farshchi YA, Akhavan M. A new Y-based HTSC with T_c above 100 K. *Phys C: Supercond Appl.* 2009;469(22):2012-4.
11. Taviana A, Akhavan M. How T_c can go above 100 K in the YBCO family. *Eur Phys J B.* 2010;73:79-83.
12. Khosroabadi H, Rasti M, Akhavan M. Structural analysis of $Y_3Ba_5Cu_8O_{19-\delta}$ -high- T_c superconductor by ab initio density functional theory. *Phys C: Supercond Appl.* 2014;497:84-8.
13. Udomsamuthirun P, Kruaehong T, Nilkamjon T, Ratreng S. The new superconductors of YBaCuO materials. *J Supercond Nov Magn.* 2010;23:1377-80.
14. Alecu G. Crystal structures of some high-temperature superconductors. *Rom Rep Phys.* 2004;56(3):404-12.
15. Iida K, Yoshioka J, Negichi T, Noto K, Sakai N, Murakami M. Strong coupled joint for Y-Ba-Cu-O superconductors using a sintered Er-Ba-Cu-O solder. *Phys C: Supercond Appl.* 2002;378-81:622-6.
16. Haruta M, Saura K, Fujita N, Ogura Y, Ichinose A, Maeda T, et al. Relationship between vortex pinning properties and microstructure in Ba-Nb-O-doped $YBa_2Cu_3O_y$ and $ErBa_2Cu_3O_y$ films. *Phys C: Supercond Appl.* 2013;494:158-62.

17. Horii S, Horide T, Matsumoto K, Ozaki T, Ichino Y, Mukaida M, et al. Critical current properties at low angle grain boundaries in $\text{ErBa}_2\text{Cu}_3\text{O}_y$ films. *Phys C: Supercond Appl.* 2008;468(15-20):1670-3.
18. Kruaehong T, Sujinnapram S, Nilkamjon T, Ratreng S, Udomsamuthirun P. Synthesized and characterization of $\text{YBa}_2\text{Cu}_3\text{O}_y$, $\text{Y}_3\text{Ba}_5\text{Cu}_8\text{O}_y$, and $\text{Y}_7\text{Ba}_{11}\text{Cu}_{18}\text{O}_y$ superconductors by planetary high-energy ball-milling. *J Aust Ceram Soc.* 2017 Apr;53:3-10.
19. Rodriguez-Carvajal J. Program Fullprof. Laboratoire Léon Brillouin (CEA-CNRS), Version. 1990;3.
20. Kita R, Kato S, Nakamura T, Miura O, Teranishi R, Yasunaga S, et al. Stability of barium oxides in $\text{REBa}_2\text{Cu}_3\text{O}_y$ superconductors. *Phys C: Supercond Appl.* 2008;468(15-20):1391-4.
21. Hassan M, Yahya AK. Influence of hot-spot temperature on oxygen sensing response behavior of Er123 ceramic rods with hot spot. *J Alloys Comp.* 2010;499(2):206-11.
22. Nazarova EK, Nenkov K, Fuchs G, Müller KH. Effects of calcium substitution on the superconducting properties of $\text{R}_{1-x}\text{Ca}_x\text{Ba}_2\text{Cu}_3\text{O}_z$ (R=Eu, Gd, Er; $0 \leq x \leq 0.3$) polycrystalline samples. *Phys C: Supercond Appl.* 2006;436(1):25-31.
23. Nedeltcheva T, Costadinova L, Simeonova P, Lovchinov V. Rapid and simple spectrophotometric determination of oxygen stoichiometry in YBCO superconducting materials. *Anal Chim Acta.* 1996;336(1-3):223-6.
24. Málková Z, Novák J, Hamplová V, Pokorná Z. Determination of the oxygen balance in oxide superconductors by a photometric method. *Fresenius J Anal Chem.* 1993;347:478-9.
25. Nedeltcheva T, Vladimirova L. Spectrophotometric determination of oxygen stoichiometry in YBCO superconducting bulk samples. *Anal Chim Acta.* 2001;437(2):259-63.
26. Liu L, Dong C, Zhang J, Chen H, Chen L. A simple volumetric method for oxygen content determination in high- T_c doped YBCO compositions. *Phys C: Supercond Appl.* 2002;383(1-2):17-22.
27. Ono A. A crystallographic study on $\text{Ba}_2\text{YCu}_3\text{O}_{7-y}$. *Japanese J Appl Phys.* 1987;26(7A):L1223.
28. Naito T, Fujishiro H, Iida K, Murakami M. Anisotropic thermal conductivity of Er-Ba-Cu-O bulk superconductors. *Phys C: Supercond Appl.* 2008;468(15-20):1428-30.
29. 399-1496 and 40-0159-JCPDS-International Centre for Diffraction Data.
30. Bakar MF, Yahya AK. Distinct effects of Al^{3+} substitution at Cu-site and Al_2O_3 addition on step-like elastic anomalies and electron-phonon coupling constant in $\text{EuBa}_2\text{Cu}_3\text{O}_{7-\delta}$ superconductors. *J Alloys Comp.* 2010;490(1-2):358-65.
31. Bianconi A, De Santis M, Di Cicco A, Flank AM, Lagarde P. Symmetry of the itinerant $3d^9$ ligand hole induced by doping in high T_c superconductors by polarized Cu L_3 XAS. *Phys B: Condens Matter.* 1989;158(1-3):443-5.
32. Benzi P, Bottizzo E, Rizzi N. Oxygen determination from cell dimensions in YBCO superconductors. *J Cryst Growth.* 2004;269(2-4):625-9.

33. Feng J, Lu Y, Zhou L, Zhang P, Xu X, Chen S, et al. The study on melting behavior of precursor powders for powder melting processed $\text{YBa}_2\text{Cu}_3\text{O}_{7-x}$ superconductors. *Phys C: Supercond Appl.* 2007;459(1-2):52-5.
34. Kim CJ, Kim KB, Jee YA, Kuk IH, Hong GW. Effects of the heating rate on conversion of the precursor powders used for melt processes into $\text{YBa}_2\text{Cu}_3\text{O}_{7-y}$. *J Mater Res.* 1999;14(4):1212-20.
35. Langhorn J, McGinn PJ. Improved microstructural characteristics in $\text{YBa}_2\text{Cu}_3\text{O}_{7-x}$ thick films prepared by a modified powder melt process route. *Phys C: Supercond Appl.* 1999;312(3-4):169-78.
36. Nakajima S, Kikuchi M, Syono Y, Oku T, Shindo D, Hiraga K, et al. Synthesis of bulk high T_c superconductors of $\text{TlBa}_2\text{Ca}_{n-1}\text{Cu}_n\text{O}_{2n+3}$ ($n=2-5$). *Phys C: Supercond Appl.* 1989;158(3):471-6.